JACS
JOURNAL OF THE AMERICAN CHEMICAL SOCIETY

Article

pubs.acs.org/JACS

Highly Ordered Dielectric Mirrors via the Self-Assembly of Dendronized Block Copolymers

Victoria A. Piunova, Garret M. Miyake, Christopher S. Daeffler, Raymond A. Weitekamp, and Robert H. Grubbs*

Arnold and Mabel Beckman Laboratories for Chemical Synthesis, Division of Chemistry and Chemical Engineering, California Institute of Technology, Pasadena, California 91125, United States

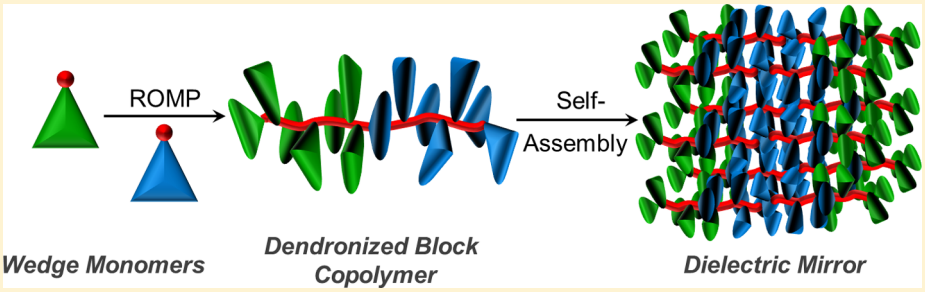

ABSTRACT: Dendronized block copolymers were synthesized by ruthenium-mediated ring-opening methathesis polymerization of *exo*-norbornene functionalized dendrimer monomers, and their self-assembly to dielectric mirrors was investigated. The rigid-rod main-chain conformation of these polymers drastically lowers the energetic barrier for reorganization, enabling their rapid self-assembly to long-range, highly ordered nanostructures. The high fidelity of these dielectric mirrors is attributed to the uniform polymer architecture achieved from the construction of discrete dendritic repeat units. These materials exhibit light-reflecting properties due to the multilayer architecture, presenting an attractive bottom-up approach to efficient dielectric mirrors with narrow band gaps. The wavelength of reflectance scales linearly with block-copolymer molecular weight, ranging from the ultraviolet, through the visible, to the near-infrared. This allows for the modulation of photonic properties through synthetic control of the polymer molecular weight. This work represents a significant advancement in closing the gap between the precision obtained from top-down and bottom-up approaches.

INTRODUCTION

Materials that can selectively control light by efficient reflection, directed propagation, or enhanced confinement have numerous applications as optical elements and devices.[1,2] Photonic crystals (PCs) are a class of nanostructured materials with tunable reflection due to their periodic dielectric function, which creates a photonic band gap where there are no allowed frequencies at which light can propagate through the material.[1,2] The simplest 1D PC architecture, termed a dielectric mirror, is constructed from alternating layers of a low and a high refractive index material.[1] The wavelength of reflected light (λ) is proportional to the domain size (d) and the refractive index (n) of the layers [$m\lambda = 2(d_1n_1 + d_2n_2)$].[1] Conventional methods to fabricate dielectric mirrors utilize top-down approaches, such as layer-by-layer depositions and coextrusion.[3] These approaches can produce highly precise structures but require complex setups and high costs. Recently, we have been focusing on the bottom-up approach of block-copolymer (BCP) self-assembly as an inexpensive and simple alternative route to dielectric mirrors with an ultimate goal of making paintable PCs.[4] Although lacking in precision, BCPs remain attractive as dielectric mirrors because their materials properties can be synthetically controlled to produce materials with tailored chemical, mechanical, and optical properties. Additionally, BCPs are a class of soft materials that can be shaped, molded, or applied to any geometric specification.[5]

Chain entanglement is a fundamental characteristic of polymers that greatly influences their bulk materials properties. Chain entanglement also presents an energetic barrier for the self-assembly of BCPs that slows the rate of equilibration to ordered morphologies. Furthermore, it complicates the synthesis of ultrahigh molecular weight (MW) polymers and generally impedes them from assembling to large domain sizes necessary to interact with long wavelength visible light.[6] Thus, most BCP-based PCs do not have high enough MWs or cannot overcome chain entanglement to an extent that allows them to assemble to long-wavelength-reflecting PCs. Traditionally, BCP-based PCs reflect wavelengths of light as long as green,[7] and domain swelling with solvents[8] or homopolymers[9] can enable interaction with longer wavelengths. Our strategy to overcome this hurdle has been to exploit polymer architectures with reduced chain entanglement to minimize the energetic barrier for reorganization and thus facilitate self-assembly.

One polymer architecture that is known to have a reduced degree of chain entanglement is the molecular brush

Received: August 6, 2013

dx.doi.org/10.1021/ja4081502 | J. Am. Chem. Soc. XXXX, XXX, XXX–XXX

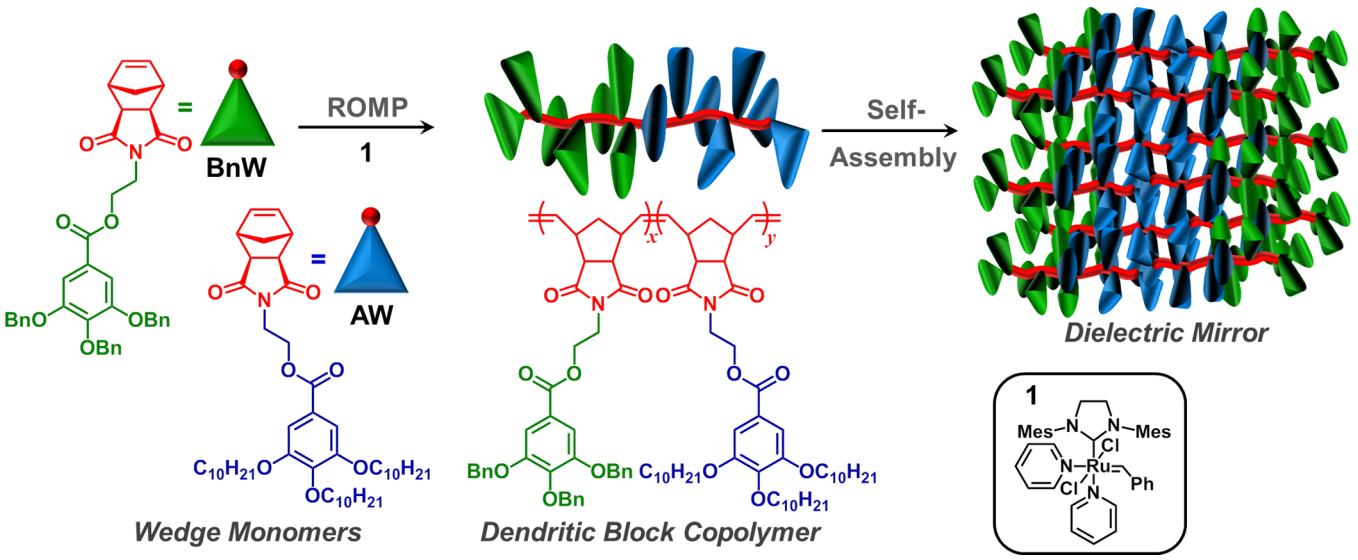

Figure 1. Structures of wedge-type monomers and their ROMP to dendronized BCPs. The schematic represents the corresponding synthesis and self-assembly to narrow bandwidth dielectric mirrors.

copolymer.[10] This architecture is composed of a sterically congested array of low MW, polymeric side chains that are unified through a common main chain. The steric interactions between the densely packed polymeric repeat units enforce the polymeric main chain to adopt a highly elongated conformation with drastically reduced entanglement.[11] Molecular brush copolymers can be constructed via grafting-from, grafting-to, or grafting-through procedures. Our interest in this field has been in the grafting-through approach, utilizing ruthenium-mediated ring-opening metathesis polymerization (ROMP)[12] of *exo*-norbornene functionalized low-MW polymers to produce ultrahigh-MW molecular brush BCPs.[13] This strategy ensures quantitative grafting density and promotes the rapid self-assembly of highly congested brush BCPs to long wavelength reflecting dielectric mirrors.[4] The brush BCPs assemble in a manner that the side chains align parallel with the lamellae, and the resulting domain size is directly modulated by the degree of polymerization through the polymer main chain, while the MW of the side chain has a much lesser impact on the domain size.[14] Thus, the peak wavelength of reflection (λ_{max}) of these materials can be predictably and precisely tuned by adjusting the degree of polymerization of the polymer main chain. Despite this capability, the bandwidths of the PCs are somewhat large and broaden with increasing λ_{max}, which inhibits their potential in applications where more precision is a requirement.[4] The ability to produce photonic crystals with controlled bandwidths is necessary for specific applications. For example, IR reflecting windows target a broad bandwidth (several hundred nanometers) to reject all nonvisible light from passing while filter or display applications call for a bandwidth of a few nanometers. This report makes a significant advancement in improving the fidelity of BCP dielectric mirrors, which results in a narrowing of the bandwidth, further enhancing their application potential.

We partially attribute the broad bandwidth in our previous systems to the nonuniform domain sizes achieved through BCP self-assembly. Within the molecular brush BCP architecture there exist three polydisperse components: the two different polymeric repeat units and the unifying polymeric main chain. Although polydispersity is known to enhance the self-assembly of linear BCPs to uniform morphologies,[15] we hypothesized that minimizing the elements of polydispersity in the polymers could enable the fabrication of more uniform and efficient dielectric mirrors. Despite the fact that the polymeric side chains align parallel with the lamellae, their dispersity could influence nonuniform packing, promoting lamellae curvature, domain size variability, and bandwidth broadening. Additionally, near the polymer chain ends the degree of steric congestion is reduced and the polymeric side chains become perpendicular to the lamellae. In this region the polydisperse polymeric side chains could further increase the dispersity in the lengths of the brush BCPs, leading to nonuniform assembly. Intuitively, it would be assumed that main-chain dispersity would have the greatest impact on the ability of the polymer to assemble to highly ordered morphologies. However, we have recently shown that main-chain dispersity is not a large deterrent, as blending two different MW brush BCPs (with identical side chains and different degrees of main-chain polymerization) can afford well-ordered morphologies where the domain sizes scale with the weight incorporation of the two components.[4c] Regardless, in the context of precision dielectric mirrors, domain size dispersity must be eliminated.

Here we explore the possibility of utilizing discrete monomers that can still produce BCPs with a highly elongated, rigid polymer architecture to reduce the dispersity in the system to increase the fidelity of the dielectric mirrors. It has been demonstrated that dendronized polymers exhibit a minimal degree of chain entanglement due to the steric repulsion between pendant monodisperse wedge side groups.[16] Thus, we believed dendronized polymers to be an ideal platform to test our hypothesis. Additionally, as the molar mass of a dendritic monomer can be considerably less than a macromonomer, an equivalent degree of polymerization within the main chain for both types of polymers would produce dendronized polymers with a significantly reduced MW in comparison to brush BCPs. The reduced MW of the dendronized polymer would presumably increase diffusion rates and enhance the rate of self-assembly. Here we report the sequential ROMP of *exo*-norbornene functionalized wedge-type monomers to dendronized BCPs and their self-assembly to highly ordered stacked

dx.doi.org/10.1021/ja4081502 | J. Am. Chem. Soc. XXXX, XXX, XXX−XXX

lamellar nanostructures with light reflecting properties (Figure 1).

RESULTS AND DISCUSSION

In order to synthesize BCPs with pendant dendritic groups we designed two norbornene wedge-type monomers functionalized with decyl (**AW**) and benzyl ether groups (**BnW**) (Figure 1). Monomers **AW** and **BnW** are AB_3-type, Newkome dendrimers where branches radiating from the central core constitute one complete generation in the dendrimer core.[17,18] The **AW** and **BnW** monomers were synthesized in high yields.[19] The ROMP of the wedge monomers was efficient over a broad range of monomer to catalyst ratios, ranging from 200:1 to 2000:1, producing polymers with MWs (weight average MW = M_w) ranging from M_w = 427 to 2932 kDa while low polydispersity indices (PDIs) (PDI = 1.01−1.27) (Table 1)

Table 1. Summary of the ROMP of BnW and AW Mediated by 1[a]

monomer (M)	[M]:[1]	conversion (%)[b]	time (min)	M_w (kDa)[c]	PDI (M_w/M_n)[c]
BnW	200:1	97	5	427	1.01
BnW	500:1	86	30	1539	1.15
BnW	1000:1	99	40	2077	1.27
BnW	1500:1	99	40	2358	1.16
BnW	2000:1	99	40	2932	1.19
AW	200:1	96	5	390	1.03

[a]Polymerizations were performed in 2.00 mL of THF at ambient temperature, [**Bn(A)W**] = 0.18 mM. [b]Determined by ^{1}H NMR. [c]Determined by light scattering.

were maintained. After demonstrating the efficient ROMP of **BnW** and **AW**, we proceeded to synthesize well-defined BCPs by addition of **AW** after the polymerization of **BnW** had been completed. The dendronized BCPs were isolated in high yields, with MWs ranging from 480 to 3340 kDa and low PDIs (PDI = 1.05−1.23) (Table 2). All BCPs had nearly equimolar incorporation of each monomer, as determined by ^{1}H NMR.

To investigate the ability of the BCPs to assemble to dielectric mirrors, we prepared thin films on glass slides by controlled evaporation from dichloromethane (DCM) solutions (concentration = 2 g/L). The fabricated films visually appeared transparent (M_w = 480 kDa), brightly colored [M_w = 570 kDa (violet) and 1250 kDa (red)], or slightly translucent (M_w = 1390, 1940 kDa). To quantify the light-reflecting properties of these materials, reflectance spectra were recorded on a spectrophotometer with an integrating sphere diffuse reflectance accessory (Table 2, Figure 2). The BCP with the lowest MW (M_w = 480 kDa) demonstrated a high-intensity

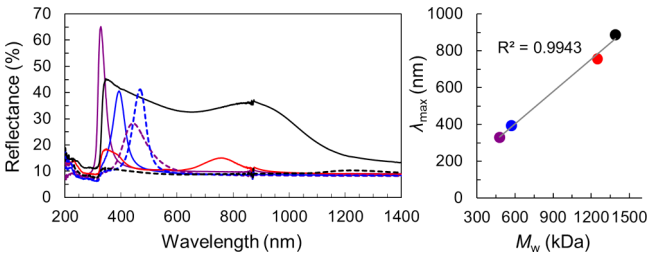

Figure 2. (Left) Plot of reflectance as a function of wavelength for thin films of the dendronized BCPs before (solid line) and after (dashed line) thermal annealing. Color scheme corresponds to the BCP MW, where M_w = 480 kDa (purple), 570 kDa (blue), 1250 kDa (red), 1390 kDa (black). Samples were prepared by controlled evaporation from DCM solutions (2 g/L) and annealed for 24 h at 100 °C under vacuum. The plot on the right demonstrates a linear correlation between λ_{max} of the primary reflectance peak and the molecular weight of the dendronized BCPs.

(65.5%), narrow bandwidth with λ_{max} of 330 nm. The brightly colored violet film (M_w = 570 kDa) also showed a narrow reflectance profile with λ_{max} = 400 nm. The red-reflecting film (M_w = 1250 kDa) exhibited a broad profile with λ_{max} = 768 nm. The film fabricated from the polymer with M_w = 1390 kDa reflected light in the near IR (λ_{max} = 1390 nm). Polymers with higher MWs did not reflect light.

Most importantly, the films fabricated from the dendronized BCPs possessed significantly narrower bandwidths than our previously reported isocyanate brush BCPs with comparable λ_{max}.[4] To directly compare the bandwidths of these dendronized BCP dielectric mirrors with our previously reported results, we calculated the gap−midgap ratio (GMR) by dividing the measured full width at half the λ_{max} (fwhm = $\Delta\lambda$) by λ_{max} (Table 3). The GMRs of the dielectric mirrors

Table 3. Comparison between Bandwidths of Dendronized BCPs and Isocyanate Brush BCPs

dendronized BCPs			brush BCP		
M_w (kDa)[a]	λ_{max} (nm)[b]	GMR (%)[c,d]	M_w (kDa)[a]	λ_{max} (nm)[b]	GMR (%)[c]
480	330	9 (5)	1512	334	17
570	393	13 (4)	2918	511	25
1250	768	18 (2)	4167	664	27

[a]Determined by light scattering. [b]Determined by spectrophotometer with integrating sphere. [c]GMR = gap−midgap ratio, determined by fwhm/λ_{max}. [d]The number in parentheses represents the theoretical values of the gap−midgap ratio with zero dispersity.

Table 2. Summary of the Copolymerization of BnW and AW Mediated by 1[a]

[**BnW**]:[**AW**]:[**1**]	M_w (kDa)[b]	PDI (M_w/M_n)[b]	**BnW** (mol %)[c]	yield (%)	λ_{max} (nm)[d]	λ_{max} (nm) annealed[d]
200:200:1	480	1.05	49.7	98.2	330	440
350:350:1	570	1.05	52.0	94.0	393	468
500:500:1	1250	1.10	49.2	98.0	757	960
750:750:1	1390	1.24	51.3	97.0	888	1223
1000:1000:1	1940	1.32	52.6	95.5		
1500:1500:1	2900	1.30	51.2	97.2		
2000:2000:1	3340	1.23	50.7	96.4		

[a]Polymerizations performed in 2.00 mL of THF at ambient temperature, [**BnW**] = [**AW**] = 0.18 mM. [b]Determined by light scattering. [c]Determined by ^{1}H NMR. [d]Determined by spectrophotometer with integrating sphere.

dx.doi.org/10.1021/ja4081502 | J. Am. Chem. Soc. XXXX, XXX, XXX−XXX

produced from dendronized BCPs were much smaller (GMR = 9−18%) than from the isocyanate-based BCPs[4b,c] (GMR = 17−27%) for dielectric mirrors that reflected light across the visible spectrum (λ_{max} = 334−768 nm). To compare the current dielectric mirrors with theoretically perfect reflectors, we computationally calculated the GMRs for dielectric mirrors possessing identical refractive indices as the dendronized BCPs but no layer thickness dispersity (vide infra). The perfect dielectric mirrors with identical λ_{max} as the dendronized BCPs had GMRs ranging from 5 to 2%.

We attribute the striking difference between the BCP systems to the fact that the polydispersity in the side groups was eliminated by replacing macromolecular repeat units with well-defined discrete groups, yielding more unified "building blocks" for the formation of highly ordered stacked lamellar morphologies. Additionally, the reduced polymer MW for dendronized BCPs, because of the lower MW of the repeat unit, most likely enables faster diffusion and assembly. In both systems, as the MW of the BCPs is increased, bandwidth broadening is observed, suggesting increased disorder in the bulk morphology. In order to overcome the kinetics for reorganization, the samples were annealed at 100 °C for 24 h. Thermal annealing induced a noticeable red shift ($\Delta\lambda_{max}$ varying from 75 to 345 nm) along with increased bandwidth broadening and decreased reflectance intensity (Figure 2, dashed lines) for samples with MW ranging from 480 to 1390 kDa (vide infra).

It is established that for 1D photonic crystals, the wavelength of reflected light is directly proportional to the domain spacing, which in turn is related to the MW of the polymer.[6] A strictly linear dependence (R^2 = 0.996) between the λ_{max} of the primary reflectance peak and the molecular weight was observed for dendronized BCPs (Figure 2), which is in accord with our previously reported systems.[4] These data are in contrast to linear polymer analogs, where the domain size is theoretically proportional to $MW^{2/3}$.[20] This unique behavior of brush or dendronized BCPs originates from the rigid architectures that exhibit a reduced degree of chain entanglement. As a result, the assembly to large domain sizes is achieved through the incorporation of a fewer number of monomer repeat units than standard random-coil BCPs.[21]

To further support the origin of the reflecting properties in dendronized BCPs, we performed transfer matrix simulations[22] to generate reflectance spectra for the dielectric mirrors (Figure 3). The simulation parameters were determined from spectroscopic ellipsometry, SEM cross sections, and reflectance data. Dispersity in the domain thicknesses and partial phase decoherence were incorporated to account for disorder in the multilayer.[23] A detailed description of the simulation procedure can be found in our previous report.[4a] The 1D transfer matrix simulations coincided with the experimentally obtained reflection spectra for all the dielectric mirrors (M_w = 480−1250 kDa). Overall, modeling results support that a multilayer stack is obtained through the rapid self-assembly of the dendronized BCPs, giving rise to 1D photonic crystals.

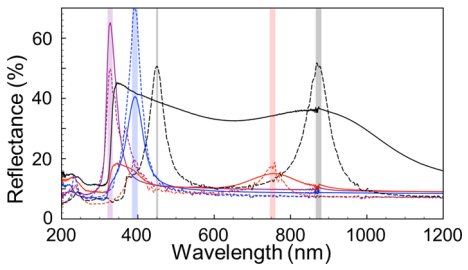

Figure 3. Plot of reflectance as a function of wavelength for dielectric mirrors fabricated from the dendronized BCPs with M_w = 480 kDa (purple), 570 kDa (blue), 1250 kDa (red), 1390 kDa (black). Dashed lines represent corresponding simulated spectra. The shaded regions represent photonic bandgaps simulated for perfectly alternating multilayers with no layer thickness dispersity.

To gain insight into the decreased bandwidths of these materials, we investigated the morphology of the films produced from DCM solutions by controlled evaporation. Cross sections of freeze-fractured films were stained with RuO_4 and examined by scanning electron microscopy (SEM). For the films produced by dendronized BCPs with MW lower than 1390 kDa, stacked lamellar morphologies were observed, as expected for the symmetric BCPs[24] (Figure 4a−c). Remarkable long-range order was observed throughout the entire bulk of the film, ranging from ∼100−200 uniform layers of alternating domains for the samples with M_w = 480 and 570 kDa (Figure 4a,b). These multilayer films show unprecedented order for BCPs in this size regime. Unfortunately, an increase in MW resulted in a rapid loss in ordering (Figure 4c,d), which was attributed to the dominating influence of chain entanglement that increases the energetic barrier for reorganization.

Comparison of the SEM cross sections before and after annealing (Figure 5) revealed some improvement in long-range order for samples with M_w = 1390 and 1940 kDa samples, in addition to lamellae thickening (1.3 times on average) for all samples. A significant overall evolution in morphology was detected for the film prepared from the BCP with M_w = 1390 kDa (Figure 5i). Initially, a poorly defined morphology, consisting of only a few domains resembling lamellae, was observed at the polymer−air interface. After annealing, stacked lamellae with domain sizes ranging between 380 and 400 nm were observed.

The film produced from the highest MW polymer (M_w = 1940 kDa) also demonstrated a drastic change in morphology. The original sample produced by controlled evaporation from DCM lacked long-range order and exhibited scattered elongated "raspberry-like" (∼1−1.5 μm long and ∼0.25 μm wide) features (Figure 5e). Upon annealing, an overall reorganization to a somewhat periodic arrangement, resembling a cylindrical morphology, was observed (Figure 5j). Similarly, the raspberry-like features were noted for the 1390 kDa sample at the polymer−substrate interface before thermal annealing. These similarities suggest that before the system reaches the thermodynamic minimum, corresponding to a lamellar morphology, it undergoes a series of metastable states, which become kinetically trapped with the high MW polymers. Even extended annealing (120 h) was unable to annihilate the morphological disorder for the polymer with M_w = 1940 kDa. The lack of morphological order for the ultrahigh-MW dendronized BCPs explains their lack of light reflecting properties. SEM analysis revealed a minimal change in morphology, which remotely resembled stacked lamellae. We hypothesize that the lamellar morphology evolution occurs through several stages, proceeding through a disordered morphology into a lower energy, metastable morphology, en route to the final thermodynamic minimum.[25] This reorganization becomes exceedingly slow with an increase in the BCP MW. The combination of the reflectance and SEM analysis suggest that the reduced MW of dendronized BCPs, in

dx.doi.org/10.1021/ja4081502 | J. Am. Chem. Soc. XXXX, XXX, XXX−XXX

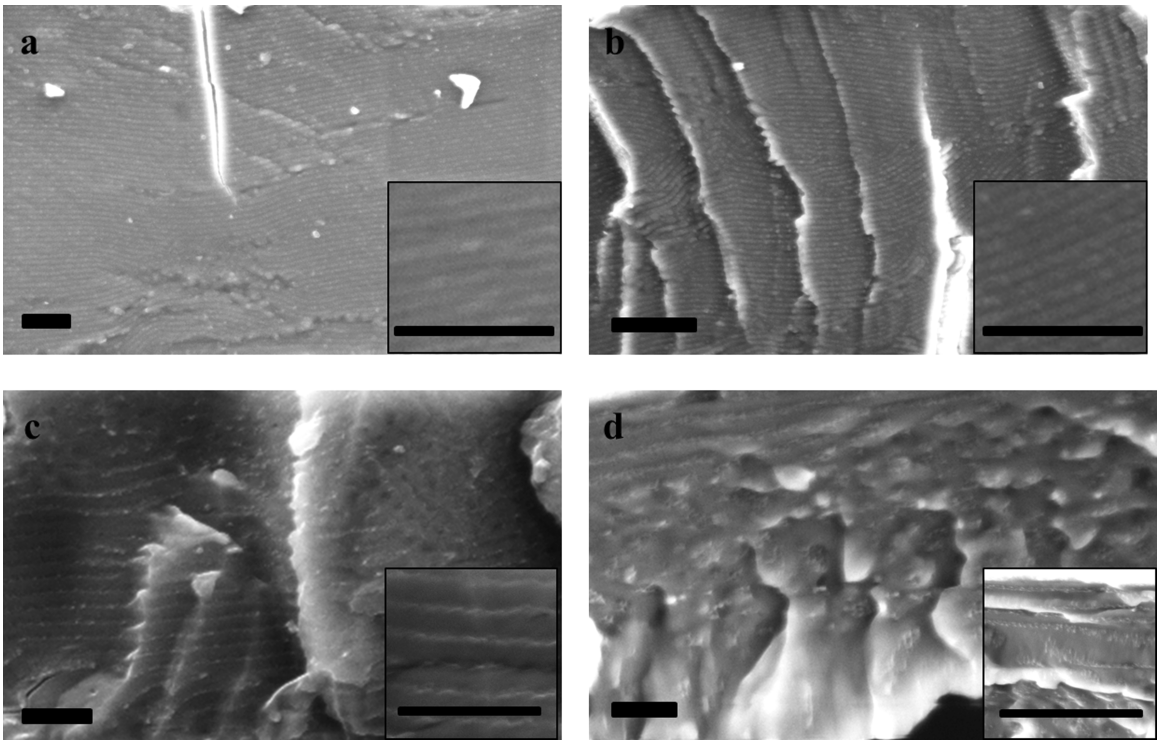

Figure 4. SEM cross sections of dendronized BCPs films prepared by controlled evaporation from DCM with M_w = 480 (a), 570 (b), 1250 (c), and 1390 (d) kDa. Scale bar = 1 μm.

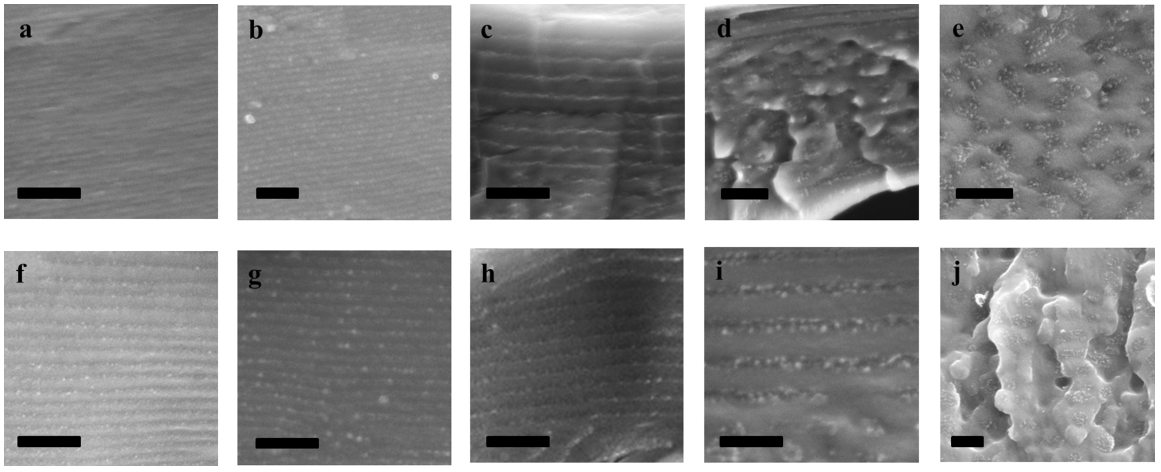

Figure 5. SEM cross sections of dendronized BCPs films prepared by controlled evaporation from DCM with M_w = 480 kDa (a, f), 570 kDa (b, g), 1250 kDa (c, h), 1390 kDa (d, i), and 1940 kDa (e, j). Scale bar = 1 μm.

comparison to brush BCPs, allows their more rapid self-assembly to highly ordered dielectric mirrors. However, the less rigid architecture of dendronized BCPs experiences a higher degree of chain entanglement, which inhibits the ultrahigh-MW polymers from rapidly reaching equilibrium, instead trapping them in a metastable state. Taking into account the annealing-induced morphological evolution observed by SEM, we attempt to explain the changes in the reflectance profiles of dendronized BCPs upon annealing. The shift in λ_{max} is caused by the increase in domain spacing induced by enthalpy-driven thickening of lamellae. However, the thickening was not uniform throughout the bulk of the material, resulting in the domain dispersity and the broadening of the reflectance peak.

CONCLUSIONS

We have synthesized a series of well-defined dendronized BCPs with MWs ranging from 480 to 3340 kDa. Rapid self-assembly of these BCPs from a volatile solvent afforded one-dimensional periodic nanostructured materials capable of reflecting light across the visible spectrum from the UV, through the visible, to the near-IR. The dielectric mirrors fabricated from dendronized BCPs demonstrated extremely narrow bandwidths of high intensity. The highly ordered nanostructures in this size regime have not been previously obtained via the self-assembly of BCPs. This work closes the gap between the precision obtained from bottom-up and top-down approaches for the fabrication of synthetic photonic crystals. With the ability to fabricate high-fidelity multilayers under ambient conditions through the self-

dx.doi.org/10.1021/ja4081502 | J. Am. Chem. Soc. XXXX, XXX, XXX–XXX

assembly of BCPs, we are working to develop paintable, functional, and tunable optical elements.

EXPERIMENTAL SECTION

Materials and Methods. $(H_2IMes)(PPh_3)(Cl)_2RuCHPh$ was received as a research gift from Materia Inc. and was converted to **1** via literature procedure.[26] *N*-(hydroxyethyl)-cis-5-norbornene-exo-2,3-dicarboximide (**2**) was prepared according to literature procedure.[27] All other chemicals were purchased from Sigma-Aldrich. Solvents were purified by passage through solvent purification columns and further degassed with argon.[28] All polymerizations were performed in a nitrogen-filled glovebox in 20 mL scintillation vials. NMR spectra were recorded on a Varian Inova 500 MHz spectrometer. Chemical shifts were referenced to internal solvent resonances and are reported as parts per million relative to tetramethylsilane. High-resolution mass spectra were provided by the California Institute of Technology Mass Spectrometry Facility. Polymer molecular weights were determined by multiangle light-scattering (MALS) gel permeation chromatography (GPC), with THF as the eluent, using a miniDAWN TREOS light-scattering detector, a Viscostar viscometer, and an OptilabRex refractive index detector, all from Wyatt Technology. An Agilent 1200 UV−vis detector was also present in the detector stack. Absolute molecular weights were determined using d*n*/d*c* values calculated by assuming 100% mass recovery of the polymer sample injected into the GPC. Polymer thin films were prepared from the controlled evaporation of polymer solutions (∼2 g/L) in dichloromethane onto glass slides that had been previously washed with methanol and hexane. After the solvent was allowed to evaporate, the samples were dried under vacuum overnight. SEM images were taken on a ZEISS 1550 VP field emission SEM. Reflection measurements were performed on a Cary 5000 UV/vis/NIR spectrophotometer, equipped with an integrating sphere diffuse reflectance accessory (Internal DRA 1800). All measurements were referenced to a LabSphere Spectralon 99% certified reflectance standard. The samples were illuminated through a Spectralon-coated aperture with a diameter of 1 cm, with a beam area of approximately 0.5 cm^2. The samples were scanned at a rate of 600 nm/min, with a 1 nm data interval, from 1800 to 200 nm, with a detector crossover (InGaAs to PMT) at 875 nm. The frequency dependent refractive indices were generously measured and fit by Ron Synowicki and Nina Hong at J.A. Woollam Co., Inc.

Synthesis of Monomers. *Methyl 3,4,5-Tris(decyloxy)benzoate (**3a**).* A 250 mL round-bottomed flask equipped with a stir bar was charged with DMF (50 mL). The solution was sparged for 30 min with argon. After sparging, the flask was sequentially charged with methyl gallate (1.9 g, 10 mmol, 1 equiv), bromodecane (10 mL, 40 mmol, 4 equiv), and potassium carbonate (8.5 g, 60 mmol, 6 equiv). The flask was then equipped with a Vigreux column and heated to 80 °C for 12 h. Upon cooling to room temperature, the reaction mixture was diluted with water (100 mL) and extracted with diethyl ether (2 × 100 mL). The combined organic phases were washed with water (100 mL) and then 50% brine (100 mL) and dried over magnesium sulfate. The combined organic phases were filtered through a plug of basic alumina. The solvent was removed by rotary evaporation to yield an oil, which became white solid **3a** (6.2 g, 9.1 mmol, 91%) in vacuo. ^{1}H NMR (500 MHz, $CDCl_3$): δ 7.25 (2H, s), 4.00 (2H, t, J = 6.5 Hz), 3.99 (4H, t, J = 6.5 Hz), 3.87 (3H, s), 1.80 (4H, quintet, J = 7 Hz), 1.73 (2H, quintet, J = 7 Hz), 1.46 (6H, quintet, J = 7 Hz), 1.38−1.19 (48H, bs), 0.87 (9H, t, 7 Hz). $^{13}C\{^1H\}$ NMR (126 MHz, $CDCl_3$): δ 166.93, 152.81, 142.36, 124.64, 107.97, 104.99, 73.48, 69.16, 52.09, 31.95, 31.93, 30.33, 29.75, 29.74, 29.73, 29.70, 29.67, 29.64, 29.57, 29.40, 29.37, 29.31, 26.08, 26.06, 22.70, 22.68, 14.14, 14.12. HRMS (FAB+): calcd 689.6084, found 689.6095.

*3,4,5-Tris(decyloxy)benzoic Acid (**3b**).* A 250 mL round-bottomed flask equipped with a stir bar was charged with **3a** (4.1 g, 6 mmol, 1 equiv), potassium hydroxide (3.4 g, 60 mmol, 10 equiv), and 95% EtOH (30 mL). The round-bottom flask was equipped with a water-cooled condenser. The suspension was refluxed (∼80 °C) for 4 h. Upon cooling, the reaction mixture thickened substantially. The solid was filtered with a Büchner funnel and washed with cold (−20 °C) 95% EtOH to give a white solid. The white solid was suspended in Et_2O (100 mL). Concentrated HCl (6 mL) was added to the ethereal suspension, followed by the precipitation of potassium chloride. Water (50 mL) was added then separated from the organic phase. The organic phase was washed with water (2 × 50 mL) and brine (1 × 50 mL) and dried over sodium sulfate. The solution was filtered and the solvent was removed by rotary evaporation to yield **3b** as a white solid (3.6 g, 5.3 mmol, 89%). ^{1}H NMR (500 MHz, $CDCl_3$): δ 7.32 (2H, s), 4.04 (2H, t, J = 7 Hz), 4.02 (4H, t, J = 7 Hz), 1.82 (4H, quintet, J = 7 Hz), 1.75 (2H, quintet, J = 7 Hz), 1.48 (6H, quintet, J = 7 Hz), 1.39−1.22 (48H, bs), 0.88 (9H, t, J = 7 Hz). $^{13}C\{^1H\}$ NMR (126 MHz, $CDCl_3$): δ 171.02, 152.85, 143.16, 123.47, 108.56, 104.99, 73.55, 69.20, 31.95, 31.93, 30.34, 29.76, 29.74, 29.73, 29.70, 29.67, 29.64, 29.57, 29.40, 29.37, 29.28, 26.08, 26.05, 22.70, 14.12. HRMS (ES): calcd 673.5771, found 673.5771.

*Alkyl Wedge Monomer (**AW**).* A 100 mL Schlenk flask equipped with a stir bar was flame-dried under vacuum. The cooled flask was backfilled with argon and charged with **3b** (3.8 g, 5.6 mmol, 1 equiv), alcohol **2** (1.3 g, 6.2 mmol, 1.1 equiv), 4-dimethylaminopyridine (66 mg, 0.56 mmol, 0.1 equiv), and CH_2Cl_2 (25 mL). The solution was cooled to 0 °C in an ice bath, with precipitation of some reagents. Dicyclohexylcarbodiimide (1.3 g, 6.2 mmol, 1.1 equiv) was added to the cooled solution, and the reaction was stirred at 0 °C for 30 min. The reaction was warmed to room temperature and stirred for 18 h. The resulting suspension was filtered and the solid was washed with CH_2Cl_2 (25 mL). Solvent was removed from the filtrate by rotary evaporation to yield very viscous oil. Ethanol (95%, 100 mL) was added to the oil and stirred for 3 h. The resulting white solid was filtered and residual solvent was removed in vacuo to yield the alkyl wedge monomer **AW** (3.4 g, 3.9 mmol, 70%). ^{1}H NMR (500 MHz, $CDCl_3$): δ 7.20 (2H, s), 6.27 (2H, t, J = 2 Hz), 4.40 (2H, t, J = 5 Hz), 4.01 (6H, t, J = 1 Hz), 3.90 (2H, t, J = 5 Hz), 3.23 (2H, m), 2.69 (1H, d, J = 2 Hz), 1.82 (4H, quintet, J = 7 Hz), 1.73 (2H, quintet, J = 7 Hz), 1.55 (1H, s), 1.48 (6H, m), 1.43−1.21 (50H, br), 0.88 (9H, t, J = 7 Hz). $^{13}C\{^1H\}$ NMR (126 MHz, $CDCl_3$): δ 177.69, 166.06, 152.81, 142.46, 137.77, 124.01, 107.98, 73.47, 69.12, 61.63, 47.85, 45.25, 42.69, 37.53, 31.95, 31.93, 30.34, 29.76, 29.74, 29.73, 29.71, 29.70, 29.67, 29.66, 29.58, 29.41, 29.40, 29.37, 29.33, 26.11, 22.70, 14.12. HRMS (ES+): calcd 864.6717, found 864.6716.

Benzyl Wedge Monomer (BnW) Synthesis. *Methyl 3,4,5-Tribenzylbenzoate (**4a**).* A 250 mL round-bottomed flask equipped with a stir bar was charged with DMF (50 mL). The solution was sparged for 30 min with argon. After sparging, the flask was sequentially charged with methyl gallate (1.9 g, 10 mmol, 1 equiv), benzyl bromide (4.8 mL, 40 mmol, 4 equiv), and potassium carbonate (8.5 g, 60 mmol, 6 equiv). The flask was then equipped with a Vigreux column and heated to 80 °C for 12 h. Upon cooling to room temperature, the reaction mixture was diluted with water (100 mL) and extracted with diethyl ether (2 × 100 mL). The combined organic phases were washed with water (100 mL) and then 50% brine (100 mL) and dried over magnesium sulfate. The combined organic phases were filtered through a plug of basic alumina. The solvent was removed by rotary evaporation to yield an oil, which became white solid **4a** (3.9 g, 98.5 mmol, 85%) in vacuo. ^{1}H NMR (500 MHz, $CDCl_3$): δ 7.48−7.44 (4H, m), 7.43−7.38 (8H, m), 7.37−7.33 (2H, m), 7.30−7.26 (3H, m), 5.16 (4H, s), 5.14 (2H, s), 3.91 (3H, s). $^{13}C\{^1H\}$ NMR (126 MHz, $CDCl_3$): δ 166.62, 152.55, 142.41, 137.43, 136.65, 128.53, 128.51, 128.17, 128.01, 127.93, 127.53, 125.21, 109.99, 109.07, 75.12, 71.23, 52.22. HRMS (FAB): calcd 454.17.80, found 454.1782.

*3,4,5-Tribenzylbenzoic Acid (**4b**).* A 250 mL round-bottomed flask equipped with a stir bar was charged with **4a** (3.9 g, 8.5 mmol, 1 equiv), potassium hydroxide (4.8 g, 85 mmol, 10 equiv), and 95% EtOH (43 mL). The round-bottom flask was equipped with a water-cooled condenser. The suspension was refluxed (∼80 °C) for 4 h. Upon cooling, the reaction mixture thickened substantially. The solid was filtered with a Büchner funnel and washed with cold (−20 °C) 95% EtOH to give a yellow solid. The solid was suspended in Et_2O (100 mL). Concentrated HCl (6 mL) was added to the ethereal suspension, followed by the precipitation of potassium chloride. The

dx.doi.org/10.1021/ja4081502 | J. Am. Chem. Soc. XXXX, XXX, XXX−XXX

suspension was filtered and washed with water. The filtrate was dissolved in acetone and dried over $MgSO_4$. Filtration and solvent removal by rotary evaporation yielded **4b** (1.85 g, 4.2 mmol, 49%). ^{1}H NMR (500 MHz, acetone-d_6): δ 7.55 (4H, d, J = 7 Hz), 7.48−7.44 (4H, m), 7.41 (4H, tt, J = 7 Hz, 1.5 Hz), 7.35 (2H, tt, J = 7 Hz, 1.5 Hz), 7.30−7.25 (3H, m), 5.23 (4H, s), 5.14 (2H, s). ^{13}C{^{1}H} NMR (126 MHz, acetone-d_6): δ 166.23, 152.62, 142.17, 137.95, 137.20, 128.41, 128.28, 128.04, 127.86, 127.73, 127.64, 125.70, 108.87, 74.59, 70.76. HRMS (FAB): calcd 441.1702, found 441.1682.

*Benzyl Wedge Monomer (**BnW**).* A 100 mL Schlenk flask equipped with a stir bar was flame-dried under vacuum. The cooled flask was backfilled with argon and charged with **4b** (1.7 g, 3.8 mmol, 1 equiv), alcohol **2** (865 mg, 4.2 mmol, 1.1 equiv), 4-dimethylaminopyridine (46 mg, 0.38 mmol, 0.1 equiv), and CH_2Cl_2 (20 mL). The solution was cooled to 0 °C in an ice bath, with precipitation of some reagents. Dicyclohexylcarbodiimide (862 mg, 4.2 mmol, 1.1 equiv) was added to the cooled solution, and the reaction was stirred at 0 °C for 30 min. The reaction was warmed to room temperature and stirred for 18 h. The resulting suspension was filtered and the solid was washed with CH_2Cl_2 (25 mL). Solvent was removed from the filtrate by rotary evaporation to yield an off-white solid. Ethanol (95%, 100 mL) was added to the oil and the mixture stirred for 3 h. The resulting white solid was filtered and residual solvent was removed in vacuo to yield **BnW** (1.9 g, 3.1 mmol, 82%). ^{1}H NMR (500 MHz, $CDCl_3$): 7.49 (4H, d, J = 8 Hz), 7.42−7.34 (10H, m), 7.29−7.26 (3H, m), 6.28 (2H, t, J = 1.6 Hz), 5.18 (4H, s), 5.14 (2H, s), 4.43 (2H, t, J = 5 Hz), 3.94 (2H, t, J = 5 Hz), 3.24 (2H, s), 2.70 (2H, s), 1.42 (1H, d, J = 10 Hz), 1.25 (1H, d, J = 10 Hz). ^{13}C{^{1}H} NMR (126 MHz, $CDCl_3$) δ 177.76, 165.76, 152.55, 142.50, 137.77, 137.45, 136.71, 128.52, 128.49, 128.16, 127.98, 127.92, 127.56, 124.60, 109.03, 75.08, 71.11, 61.86, 47.85, 45.26, 42.67, 37.50. HRMS (FAB): calcd 629.2413, found 629.2392.

Synthesis of Dendronized Homopolymers. A 20 mL vial was charged with a stir bar, 113 mg (0.18 mmol) of **BnW** or 140 mg (0.18 mmol) of **AW**, and THF (2.0 mL). With rapid stirring 10 μL of an appropriate concentration of **1** in THF was quickly added via syringe. For kinetic analysis a 0.2 mL aliquot of the reaction solution was taken at predetermined time intervals and injected into a 2.0 mL septum sealed vial, containing a solution of 25 μL of ethyl vinyl ether in 0.7 mL of THF. The aliquot was analyzed by GPC to determine the molecular weight of the polymer. After the solvent was allowed to evaporate from the vials the polymer residue was redissolved in $CDCl_3$, it was analyzed by ^{1}H NMR spectroscopy to determine the percent of monomer conversion by comparing the peaks corresponding to the wedge polymer and the unreacted monomer. The polymerization was quenched by the addition of 200 μL of ethyl vinyl ether and addition of 25 mL of methanol. The mixture was allowed to stir for 1 h, and the polymer was isolated by filtration and dried under vacuum at ambient temperature to a constant weight.

BnW homopolymer: ^{1}H NMR ($CDCl_3$, 300 MHz, 25 °C): δ 7.02−7.40 (m), 6.91 (bs), 5.12 (bs), 4.99 (m), 4.26 (bs).

AW homopolymer: ^{1}H NMR ($CDCl_3$, 300 MHz, 25 °C): 7.10−7.42 (m), 5.05 (t), 4.34 (bs), 3.97 (m), 3.8 (bs), 2.75 (bs), 1.76 (bs), 1.45 (bs), 0.86 (t).

Synthesis of Dendronized BCPs. In a nitrogen-filled glovebox a 20 mL vial was charged with a stir bar, 113 mg (0.18 mmol) of **BnW**, and 2.0 mL of THF. With rapid stirring 10 μL of an appropriate concentration of **1** in THF was quickly added via syringe. At predetermined time intervals 140 mg (0.18 mmol) of **AW** was added as a solid, and the solution was allowed to react as specified in polymerization tables. The polymerization was quenched by addition of 150 μL of ethyl vinyl ether and addition of 15 mL of methanol. The mixture was allowed to stir for 1 h and polymer was isolated and dried under vacuum at ambient temperature to a constant weight. No unreacted monomer was present in the isolated block polymer, as determined by GPC and ^{1}NMR analysis. ^{1}H NMR: ($CDCl_3$, 300 MHz, 25 °C): δ 7.02−7.40 (m), 5.40 (bs), 5.06(t), 4.3 (s), 3.97 (m), 1.77 (bs), 1.45 (bs), 1.25 (bs), 0.8 (t). dn/dc value: 0.1251.

AUTHOR INFORMATION

Corresponding Author

rhg@caltech.edu

Notes

The authors declare no competing financial interest.

ACKNOWLEDGMENTS

We gratefully acknowledge Ron Synowicki and Nina Hong at J.A. Woollam Co., Inc. for their measurement and fitting of the refractive indices of these polymers. Reflection measurements were collected at the Molecular Materials Research Center of the Beckman Institute of the California Institute of Technology. This work was supported by a Dow-Resnick Bridge Award. This research was conducted with Government support under and awarded by DoD, Air Force Office of Scientific Research, National Defense Science and Engineering Graduate (NDSEG) Fellowship (32 CFR 168a).

REFERENCES

(1) Joannopoulos, J. D.; Johnson, S. G.; Winn, J. N.; Meade, R. D. *Photonic Crystals: Molding the Flow of Light*, 2nd ed.; Princeton University Press: Princeton, NJ, 2008.

(2) (a) Ge, J.; Yin, Y. *Angew. Chem., Int. Ed.* **2011**, *50*, 1492−1522. (b) Galisteo-López, J. F.; Ibisate, M.; Sapienza, R.; Froufe-Perez, L. S.; Blanco, Á.; López, C. *Adv. Mater.* **2011**, *23*, 30−69. (c) Wang, J.; Zhang, Y.; Wang, S.; Song, Y.; Jiang, L. *Acc. Chem. Res.* **2011**, *44*, 405−415. (d) Aguirre, C. I.; Reguera, E.; Stein, A. *Adv. Funct. Mater.* **2010**, *20*, 2565−2578. (e) Moon, J. H.; Yang, S. *Chem. Rev.* **2012**, *110*, 547−574.

(3) (a) Huang, J.; Wang, X.; Wang, Z. L. *Nano Lett.* **2006**, *6*, 2325−2331. (b) Jiang, P.; Ostojic, G. N.; Narat, R.; Mittleman, D. M.; Colvin, V. L. *Adv. Mater.* **2001**, *13*, 389−393. (c) Schrenk, W. J.; Wheatley, J. A.; Lewis, R. A.; Arends, C. B. *Tappi J.* **1992**, 169−174.

(4) (a) Sveinbjörnsson, B. R.; Weitekamp, R. A.; Miyake, G. M.; Xia, Y.; Atwater, H. A.; Grubbs, R. H. *Proc. Natl. Acad. Sci. U. S. A.* **2012**, *109* (36), 14332−14336. (b) Miyake, G. M.; Weitekamp, R. A.; Piunova, V. A.; Grubbs, R. H. *J. Am. Chem. Soc.* **2012**, *134*, 14249−14254. (c) Miyake, G. M.; Piunova, V. A.; Weitekamp, R. A.; Grubbs, R. H. *Angew. Chem., Int. Ed.* **2012**, *51*, 11264−11248. (d) Xia, Y.; Olsen, B. D.; Kornfield, J. A.; Grubbs, R. H. *J. Am. Chem. Soc.* **2009**, *131*, 18525−18532.

(5) (a) Bates, F. S.; Hillmyer, M. A.; Lodge, T. P.; Bates, C. M.; Delaney, K. T.; Fredrickson, G. H. *Science* **2012**, *336*, 434−440. (b) Park, C.; Yoon, J.; Thomas, E. L. *Polymer* **2003**, *44*, 6725−6760.

(6) Edrington, A. C.; Urbas, A. M.; DeRege, P.; Chen, C. X.; Swager, T. M.; Hadjichristidis, N.; Xenidou, M.; Fetters, L. J.; Joannopoulos, J. D.; Fink, Y.; Thomas, E. L. *Adv. Mater.* **2001**, *3*, 421−425.

(7) (a) Hustad, P. D.; Marchand, G. R.; Garcia-Meitin, E. I.; Roberts, P. L.; Weinhold, J. D. *Macromolecules* **2009**, *42*, 3788−3794. (b) Rzayev, J. *Macromolecules* **2009**, *42*, 2135−2141. (c) Runge, M. B.; Bowden, N. B. *J. Am. Chem. Soc.* **2007**, *129*, 10551−10560. (d) Yoon, J.; Mathers, R. T.; Coates, G. W.; Thomas, E. L. *Macromolecules* **2006**, *39*, 1913−1919.

(8) (a) Parnell, A. J.; Pryke, A.; Mykhaylyk, O. O.; Howse, J. R.; Adawi, A. M.; Terrill, N. J.; Fairclough, J. P. A. *Soft Mater.* **2011**, *7*, 3721−3725. (b) Yamanaka, T.; Hara, S.; Hirohatta, T. *Opt. Express* **2011**, *19*, 24583−24588. (c) Kang, C.; Kim, E.; Baek, H.; Hwang, K.; Kwak, D.; Kang, Y.; Thomas, E. L. *J. Am. Chem. Soc.* **2009**, *131*, 7538−7539. (d) Yoon, J.; Lee, W.; Thomas, E. L. *Macromolecules* **2008**, *41*, 4582−4584. (e) Kang, Y.; Walish, J. J.; Gorishnyy, T.; Thomas, E. L. *Nat. Mater.* **2007**, *6*, 957−960.

(9) (a) Urbas, A.; Sharp, R.; Fink, Y.; Thomas, E. L.; Xenidou, M.; Fetters, L. J. *Adv. Mater.* **2000**, *12*, 812−814. (b) Urbas, A.; Fink, Y.; Thomas, E. L. *Macromolecules* **1999**, *32*, 4748−4750.

(10) (a) Rzayev, J. *ACS Macro Lett.* **2012**, *1*, 1146−1149. (b) Sumerlin, B. S.; Matyjaszewski, K. In *Macromolecular Engineering:*

Precise Synthesis, Materials Properties, Applications; Matyjaszewski, K., Gnanou, Y., Leibler, L., Eds.; Wiley-VCH: Weinheim, Germany, 2007.
(11) (a) Hu, M.; Xia, Y.; McKenna, G. B.; Kornfield, J. A.; Grubbs, R. H. *Macromolecules* **2011**, *44*, 6935−6943. (b) Tsukahara, Y.; Namba, S.; Iwasa, J.; Nakano, Y.; Kaeriyama, K.; Takahashi, M. *Macromolecules* **2001**, *34*, 2624−2629. (c) Vlassopoulos, D.; Fytas, G.; Loppinet, B.; Isel, F.; Lutz, P.; Benoit, H. *Macromolecules* **2000**, *33*, 5960−5969.
(12) (a) Vougioukalakis, G. C.; Grubbs, R. H. *Chem. Rev.* **2010**, *110*, 1746−1787. (b) Leitgeb, A.; Wappel, J.; Slugovc, C. *Polymer* **2010**, *51*, 2927−2946. (c) Bielawski, C. W.; Grubbs, R. H. In *Controlled and Living Polymerizations*; Müller, A. H. E., Matyjaszewski, K., Eds.; Wiley-VCH: Weinheim, Germany, 2009; pp 297−342; (d) Bielawski, C. W.; Grubbs, R. H. *Prog. Polym. Sci.* **2007**, *32*, 1−29. (e) Slugovc, C. *Macromol. Rapid Commun.* **2004**, *25*, 1283−1297.
(13) Xia, Y.; Kornfield, J. A.; Grubbs, R. H. *Macromolecules* **2009**, *42*, 3761−3766.
(14) Weiyin, G.; Huh, J.; Hong, S. W.; Sveinbjornsson, B. R.; Park, C.; Grubbs, R. H.; Russel, T. P. *ACS Nano* **2013**, *7*, 2551−2558.
(15) (a) Darling, S. B. *Prog. Polym. Sci.* **2007**, *32*, 1152−1204. (b) Lynd, N. A.; Meuler, A. J.; Hillmyer, M. A. *Prog. Polym. Sci.* **2008**, *33*, 875−893. (c) Lynd, N. A.; Hillmyer, M. A. *Macromolecules* **2005**, *38*, 8803−8810. (d) Widin, J. M.; Kim, M.; Schmitt, A. K.; Han, E.; Gopalan, P.; Mahanthappa, M. K. *Macromolecules* **2013**, *46*, 4472−4480.
(16) (a) Schlüter, A. D.; Rabe, J. P. *Angew. Chem., Int. Ed.* **2000**, *39*, 864−883. (b) Zhang, A.; Shu, L.; Bo, Z.; Schlüter, A. D. *Macromol. Chem. Phys.* **2003**, *204*, 328−339. (c) Boydston, A. J.; Holcombe, T. W.; Unruh, D. A.; Fréchet, J. M. J.; Grubbs, R. H. *J. Am. Chem. Soc.* **2009**, *131*, 5388−5389. (d) Rajaram, S.; Choi, T.-L.; Rolandi, M.; Fréchet, J. M. J. *J. Am. Chem. Soc.* **2007**, *129*, 9619−9621. (e) Chen, Y.; Xiong, X. *Chem. Commun.* **2010**, *46*, 5049−5060.
(17) Newkome, G. R.; Kotta, K. K.; Moorefield, C. N. *J. Org. Chem.* **2005**, *70*, 4893−4896.
(18) Medina, S. H.; El-Sayed, M. E. H. *Chem. Rev.* **2009**, *109*, 3141−3157.
(19) See Experimental Section.
(20) Matsen, M. W.; Bates, F. S. *J. Polym. Sci., Part B: Polym. Phys.* **1997**, *35*, 945−952.
(21) Lee, H.; Matyjaszewski, K.; Yu-Su, S.; Sheiko, S. S. *Macromolecules* **2008**, *41*, 6073−6080.
(22) Orfanidis S. J. *Electromagnetic Waves and Antennas*; online book, retrived May 2012; http://www.ece.rutgers.edu/~orfanidi/ewa.
(23) Troparevsky, M. C.; Sabau, A. S.; Lupini, A. R.; Zhang, Z. *Opt. Express* **2010**, *18*, 24715−24721.
(24) Fredrickson, G. H.; Bates, F. S. *Annu. Rev. Mater. Sci.* **1996**, *26*, 501−550.
(25) Rastogi, S.; Spoelstra, D.; Goossens, J. G. P.; Lemstra, P. J. *Macromolecules* **1997**, *30*, 7880−7889.
(26) Love, J. A.; Morgan, J. P.; Trnka, T. M.; Grubbs, R. H. *Angew. Chem., Int. Ed.* **2002**, *41*, 4035−4037.
(27) Matson, J. B.; Grubbs, R. H. *J. Am. Chem. Soc.* **2008**, *130*, 6731−6733.
(28) Pangborn, A. B.; Giardello, M. A.; Grubbs, R. H.; Rosen, R. K.; Trimmer, F. J. *Organometallics* **1996**, *15*, 1518−1520.